An enhanced method for the determination of the ramping reserves

Citation: Muzhikyan, Aramazd, Amro M. Farid, and Kamal Youcef-Toumi. "An Enhanced Method for the Determination of the Ramping Reserves." 2015 American Control Conference (ACC) (July 2015), pp. 994-1001.

As Published: http://dx.doi.org/10.1109/ACC.2015.7170863

Publisher: Institute of Electrical and Electronics Engineers

Persistent URL: http://hdl.handle.net/1721.1/109109

Version: Author's final manuscript: final author's manuscript post peer review, without publisher's formatting or copy editing

A. Muzhikyan, A. M. Farid, and K. Youcef-Toumi, "An Enhanced Method for Determination of the Ramping Reserves," in IEEE American Control Conference, (Los Angeles, CA, USA), pp. 1–8, 2015.

An Enhanced Method for Determination of the Ramping Reserves

Aramazd Muzhikyan[1], Amro M. Farid[2] and Kamal Youcef-Toumi[3]

***Abstract*—Power generation reserves play a central role for maintaining the balance of generation and consumption. Reserves, scheduled in advance, compensate for forecast error, variability and transmission losses. However, as reserves are a costly commodity, their amount should be carefully assessed to prevent unnecessary expense. Currently, the quantity of required reserves are determined based upon *a posteriori* methods that use operator's experience and established assumptions. While these assumptions have been made out of a level of engineering practicality, they may not be formally true given the numerical evidence. The earlier "sister" paper to this work presented a method to determine the quantity of load following reserves *a priori*. This paper now uses a similar methodology to determine the quantity of *ramping* reserves.**

I. INTRODUCTION

Power balance is one of the key requirements for reliable power system operations. To that end, system operators schedule appropriate amounts of generation to meet the real-time demand. However, forecast error, load variability and transmission losses impose practical limitations on the scheduling process. Normally, this challenge is overcome with the scheduling of additional generation capacity called load following reserves. Doing so, implicitly also schedules a corresponding amount of *ramping* reserves; which are the maximum and minimum ramp rates of the dispatched generators. Generally speaking, ad-hoc empirical methods have been used to determine the *appropriate* amount of load following reserves and the development for more formal methods still remains an open research question. Furthermore, there is severe lack of methods to determine the *appropriate* amount of ramping reserves. This paper uses classification of reserves as it is defined in [1], [2].

The existing industrial practice and academic literature revolves around a similar theme. As discussed in [3], the quantity of reserves is determined *a posteriori* on the basis of historical experience of power system operation. The standard deviation of potential imbalances, σ, is determined from the forecast error or the net load variability. Then, the load following reserves are defined to cover the appropriate confidence interval in compliance with the North American Electric Reliability Corporation (NERC) balancing requirements. NERC defines the minimum score for the Control Performance Standard 2 (CPS2) equal to 90% [4]. Under the assumption of normal distribution, a 2σ confidence interval is chosen [3], [5]. Other studies have used a 3σ confidence interval [6], [7] to comply with the industry standard of 95% [8].

These industrial and academic works essentially make the following assumptions in their calculations of load following reserves for the next relevant period of time.

Assumption 1. ***Invariant Probability Density Function of Imbalances:*** *The probability density function of the power system imbalances measured over the previous period will be of the same functional shape in the next period. Normally, it is assumed that the imbalances have a normal distribution.*

Assumption 2. ***Equivalence of Standard Deviations:*** *The standard deviation of power system imbalances is equivalently determined by either the net load variability or the forecast error. Some works use variability [3], [9], [10], while others use the forecast error [7], [11]–[13].*

Assumption 3. ***Invariant Standard Deviation:*** *The standard deviation in the next period will be of the same magnitude as in the current period.*

Assumption 4. ***Non-dependence on Power System Operator Decisions & Control:*** *The standard deviation of power system imbalances does not depend on the endogenous characteristics of the power system operator decisions and control. According to Assumption 2, it depends only on variability and forecast error, which can be viewed as exogenous disturbances to the power system operation and control.*

While these assumptions have been made out of a level of engineering practicality, it is unlikely that they are formally true. Assumption 1 suggests that the power system's stochastic processes retain their characteristics from one period to the next in the form of a normal distribution, which has no numerical evidence [14]–[16]. In regards to Assumption 2, a perfectly forecasted but highly variable net load still requires more load following reserves than a modestly variable net load [17]. Similarly, a high forecast error will require greater reserves than low forecast error [17]. Therefore, the reserve requirements is more likely to depend on both variability and forecast error. Meanwhile, Assumption 3 suggests that power system does not evolve over the long term. However, variables such as the variable energy resource (VER) penetration level and capacity factor, the forecast error, the net load variability, and the resource scheduling time step all have the potential to change over the term. Finally, the recent Federal Energy Regulatory Commission (FERC) requirement to change the minimum frequency of the balancing market from 1 hour to 15 minutes suggests that power system imbalances do depend on the power system's endogenous characteristics contrary to

[1]Aramazd Muzhikyan is with the Department of Engineering Systems and Management, Masdar Institute of Science and Technology, PO Box 54224, Abu Dhabi, UAE amuzhikyan@masdar.ac.ae

[2]Amro M. Farid is with Faculty of Engineering Systems and Management, Masdar Institute of Science and Technology, PO Box 54224, Abu Dhabi, UAE afarid@masdar.ac.ae

[3]Kamal Youcef-Toumi is with Faculty of Mechanical Engineering, Massachusetts Institute of Technology, 77 Massachusetts Avenue Cambridge, MA 02139, USA youcef@mit.edu

Assumption 4. A more detailed discussion of the potential invalidity of these assumptions can be found in [17].

The earlier "sister" paper to this work [18] presented an enhanced method to determine the quantity of load following reserves *a priori* with a set of assumptions that are more closely supported by numerical evidence and analytical models. This paper now does the same; using a similar methodology to determine the quantity of *ramping* reserves. It is organized as follows. Section II provides the background of the problem and the fundamental definitions, Section III presents the methodology of the ramping reserve requirements calculation and Section IV summarizes the results and presents the future work.

II. BACKGROUND

This section provides the conceptual background necessary for the operating reserves calculation methodology presented in the following section. This consists of an introduction to power grid enterprise control model and definition of a number of fundamental terms.

A. Power Grid Enterprise Control

In this paper, power system operations are modeled as a three-layer enterprise control [19], [20] on top of the physical power grid as presented in Fig. 1. The balancing is performed through three consecutive stages, namely resource scheduling, balancing actions and regulation service. Each consecutive stage operates at a smaller timescale, that allows successive improvements of power balance. The system takes as inputs the day-ahead and short-term net load forecasts and the reserve requirements.

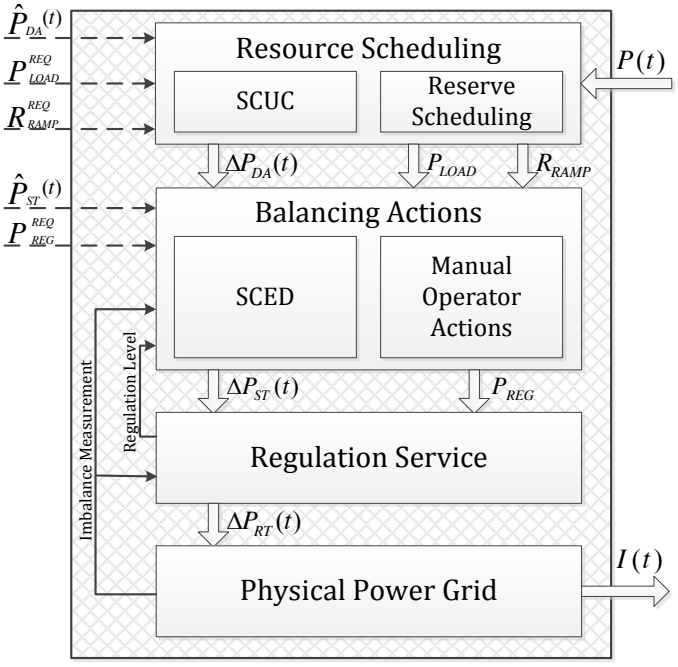

Figure 1: A three-layer power grid enterprise control model

The resource scheduling is performed by running security-constrained unit commitment (SCUC), which is formulated as a linear mixed-integer program [21]. SCUC uses the day-ahead net load forecast $\hat{P}_{DA}$ to schedule generation that meets the real-time net load $P(t)$. Since the forecast is not perfect, the actually scheduled generation and ramping capabilities do not match the real-time requirements, and $\Delta P_{DA}(t)$ imbalance remains at the SCUC output. To this end, SCUC also schedules P_{LOAD} load following and R_{RAMP} ramping reserves to mitigate the imbalance in the next stage [19], [20].

The balancing actions layer consists of a security-constrained economic dispatch (SCED) and manual operator actions. The SCED uses the short-term net load forecast $\hat{P}_{ST}(t)$ information and scheduled reserves to re-dispatch the generation in real-time. It should be noted that the imbalance at the output of this stage $\Delta P_{ST}(t)$ is smaller since SCED uses a more accurate forecast and operates at a smaller timescale. In parallel to generation dispatch, procurement of regulation reserve P_{REG} is made to mitigate the imbalance in the next stage.

The regulation service layer is based on an automatic generation control (AGC) algorithm. The AGC responds to the current imbalance level and adjusts the generation output to mitigate it. The imbalance $\Delta P_{RT}(t)$ at the output of regulation service layer is further mitigated by the load response and system inertia and the remaining imbalance $I(t)$ is used to assess system balancing performance.

B. Fundamental Definitions

In order to facilitate the usage of this work across different power systems, a number of non-dimensional quantities are introduced.

Definition 1. Penetration Level (π)*: The installed VER capacity P_V^{max} normalized by the system peak load P_L^{peak} [22]:*

$$\pi = P_V^{max} / P_L^{peak} \tag{1}$$

Definition 2. VER Capacity Factor (γ)*: The average VER output $P_V(t)$ per installed capacity taken over a period T_0 (e.g. 1 year) [18]:*

$$\gamma = \frac{\overline{P^V(t)}}{P_V^{max}} \tag{2}$$

Definition 3. Variability (A)*: Given the choice of the output $P(t)$ (e.g. the VER generation, the load, the net load), the variability is the root-mean-square of that output's rate normalized by the root-mean-square of that output [18]:*

$$A = \frac{rms\left(\mathrm{d}P(t)/\mathrm{d}t\right)}{rms(P(t))} \tag{3}$$

It is known from the literature that VER and load power spectra have distinctive shapes [23], [24]. Thus, the way to manipulate the variability of the profile while keeping its spectral shape is temporal scaling of the profile. Assume that a base profile $P_0(t)$ has a variability A_0 and $P(t)$ is defined as:

$$P(t) = P_0(\alpha t) \tag{4}$$

According to (3):

$$A = \frac{rms\left(\mathrm{d}P_0(\alpha t)/\mathrm{d}t\right)}{rms(P_0(\alpha t))} = \alpha \cdot \frac{rms\left(\mathrm{d}P_0(\alpha t)/\mathrm{d}\left(\alpha t\right)\right)}{rms(P_0(t))} = \alpha A_0 \tag{5}$$

Thus, α is the variability of the given profile normalized by the base variability A_0 [18]:

$$\alpha = \frac{A}{A_0} \tag{6}$$

Finally, it is important to introduce a number of definitions in regards to the forecast and its error. Fundamentally speaking, while the net load is a continuously varying function in time, the forecast has discrete values resolved with each scheduling time block (e.g. 1 hour). Therefore, the two quantities are inherently mismatched. Instead, the "Best Forecast" and "Best Ramping Forecast" are defined.

Definition 4. The Best Forecast*: Given the choice of the output $P(t)$ (e.g. the VER generation, the load, the net load), the best forecast value $\bar{P}_{k,T}$ is equivalent to the average value of the output during the k^{th} time block of duration T:*

$$\bar{P}_{k,T} = \frac{1}{T}\int_{kT}^{(k+1)T} P(t)\mathrm{dt} \tag{7}$$

Definition 5. The Best Ramping Forecast*: Given the choice of the output $P(t)$ (e.g. the VER generation, the load, the net load), the best ramping forecast value $\bar{R}_{k,T}$ is the best forecast change during the k^{th} time block divided by the time block duration T:*

$$\bar{R}_{k,T} = \frac{P_{k+1,T} - P_{k,T}}{T} \tag{8}$$

The forecast error definition is based on the deviation between the actual forecast and the best forecast, which in turn may be defined by various measures such as mean absolute error (MAE), mean square error (MSE) [25]. It is also often convenient to normalize the load and VER forecast errors by the peak load and the installed capacity respectively.

Definition 6. Load Forecast Error (ε_L)*: The standard deviation of the difference between the best and the actual load forecasts normalized by the peak load [18]:*

$$\varepsilon_L = \frac{\sqrt{\frac{1}{n}\sum_{k=0}^{n}\left(\bar{P}_k^L - \hat{P}_k^L\right)^2}}{P_L^{peak}} \tag{9}$$

Definition 7. VER Forecast Error (ε_V)*: The standard deviation of the difference between the best and the actual VER forecasts normalized by the installed capacity [18]:*

$$\varepsilon_V = \frac{\sqrt{\frac{1}{n}\sum_{k=0}^{n}\left(\bar{P}_k^V - \hat{P}_k^V\right)^2}}{P_V^{max}} \tag{10}$$

Finally, it is important to define a set of profiles used in the ramping reserve calculations. They may be understood graphically as shown in Fig. 2.

Definition 8. Best Generation Schedule*: A constant time series at the value of the best forecast over the given interval T:*

$$\bar{P}_T(t) = \bar{P}_{k,T},\ kT \le t \le (k+1)T \tag{11}$$

Definition 9. Forecasted Generation Schedule*: A constant time series at the value of the net load forecast over the given interval T:*

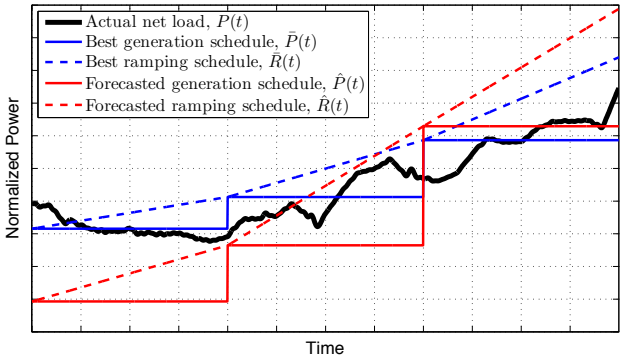

Figure 2: Actual output, forecasted profile and best forecast profile

$$\hat{P}_T(t) = \hat{P}_{k,T},\ kT \le t \le (k+1)T \tag{12}$$

Definition 10. Best Ramping Schedule*: A constant time series at the value of the best ramping forecast over the given interval T:*

$$\bar{R}_T(t) = \bar{R}_{k,T},\ kT \le t \le (k+1)T \tag{13}$$

Definition 11. Forecasted Ramping Schedule*: A constant time series at the value of the net load ramping forecast over the given interval T:*

$$\hat{R}_T(t) = \hat{R}_{k,T},\ kT \le t \le (k+1)T \tag{14}$$

This work assumes that the load and VER forecasts have zero mean error:

$$\sum_{k=0}^{n}\left(\bar{P}_k - \hat{P}_k\right) = \sum_{k=0}^{n}\left(\bar{P}_k^L - \hat{P}_k^L\right) = \sum_{k=0}^{n}\left(\bar{P}_k^V - \hat{P}_k^V\right) = 0 \tag{15}$$

It also assumes that any shifted copies of VER and load forecast errors are uncorrelated [26], i.e., for any integer m:

$$\sum_{k=0}^{n}\left(\bar{P}_k^L - \hat{P}_k^L\right)\left(\bar{P}_{k+m}^V - \hat{P}_{k+m}^V\right) = 0 \tag{16}$$

III. RAMPING RESERVE REQUIREMENT CALCULATION METHODOLOGY

As stated in the Section II, the generation and ramping scheduling process is performed based on the solution of the SCUC problem. However, in real power systems the scheduled generation *never* matches the actual required output. Three factors are identified, that affect this mismatch [18]:

- **Scheduling time step.** The SCUC problem has a limited time resolution: usually the scheduled values are given on a hourly basis. However, the real-time power output changes constantly, which makes matching of scheduled and actually required generation impossible.
- **Forecast error.** The SCUC problem is solved based on the day-ahead net load forecast. However, the real time net load output never matches the forecasted value, since each forecasting process has limited accuracy. This forecast error contributes to the mismatch.

- **Transmission losses.** The linearized SCUC problem ignores system losses in the power balance equation. However, in a real power system the losses also participate in the power balance. Absence of the loss term also increases the mismatch.

Using the profile definition above, the difference between actual consumption and the scheduled generation ramping rates can be written as follows:

$$\Delta R(t) = \frac{\mathrm{d}\left(P(t)+L(t)\right)}{\mathrm{dt}} - \hat{R}_T(t) = \\ = \left(R(t) - \bar{R}_T(t)\right) + \left(\bar{R}_T(t) - \hat{R}_T(t)\right) + \frac{\mathrm{d}L(t)}{\mathrm{dt}} \tag{17}$$

where $P(t)$ net load is the combined load and VER:

$$P(t) = P^L(t) - P^V(t) \tag{18}$$

The third term is the change rate of the transmission losses as the generation outputs and loads change. Normally, the transmission losses are about $4-8\%$ of the total active power generated [27] and stay nearly at the constant level during the operations. Thus, the third term can be ignored.

A. The Strategy

While the existing reserve requirement determination techniques are driven by Assumptions 1-4, the current paper seeks to test these assumptions and propose an analytical model that changes the reserve requirement determination framework from assumptions to equations. Similar calculations for the determination of the load following reserve requirement is presented in [18]. As the first step, an analytical expression for the standard deviation of the potential *ramping* imbalances described in (17) is derived that explicitly contains the defined dimensionless units:

$$\sigma\left(\pi, \gamma, \alpha_L, \alpha_V, \varepsilon_L, \varepsilon_V, T\right) \tag{19}$$

This expression provides an *a priori* determination of how *ramping* reserve requirements evolve as the system evolves and hence are sufficient to comprehensively test the validity of Assumptions 2-4. Next, the shape of the probability density function potential imbalances is studied under a variety of scenarios to test the credibility of Assumption 1. Such an analysis helps in the numerical determination of the required confidence multiplier β:

$$R_{RAMP} = \beta\sigma \tag{20}$$

This strategy gains further importance by virtue of the fact that the major part of the derivation of (19) is carried out in the spectral domain. Previous work in the literature has shown that the power spectra of VER generation and load have distinctive shapes [23], [24] which may be described by the very same parameters as in (19). Therefore, the method presented in this paper allows a ramping reserve calculation which may be generalized to different VER integration scenarios.

B. The Statistical Moments

This section is devoted to the calculation of the standard deviation of ramping imbalance (17). First, the average value of the imbalance is calculated straightforwardly and then a more involved calculation of the standard deviation is presented.

1) The Average Value of Ramping Imbalances: By definition, the average value of ramping imbalance in (17):

$$m = \frac{1}{T_0}\int_0^{T_0}\left(R(t) - \hat{R}(t)\right)\mathrm{dt} = \frac{1}{T_0}\int_0^{T_0} R(t)\mathrm{dt} - \frac{1}{T_0}\int_0^{nT}\hat{R}(t)\mathrm{dt} = \\ = \frac{P(T_0)-P(0)}{T_0} - \frac{1}{T_0}\sum_{k=0}^{n-1}\left[\int_{kT}^{(k+1)T}\hat{R}(t)\mathrm{dt}\right] = \frac{P(T_0)-P(0)}{T_0} - \\ - \frac{1}{T_0}\sum_{k=0}^{n-1}\left(\hat{P}_{t+1} - \hat{P}_t\right) = \frac{P(T_0)-P(0)}{T_0} - \frac{\hat{P}_n - \hat{P}_0}{T_0} \tag{21}$$

where $n = T_0/T$ is the integer number of T intervals in the data set. For a long data set m can be assumed to be zero. The calculation of the standard deviation is presented in the following section.

2) The Standard Deviation of Imbalances: By definition, the standard deviation of ramping imbalance (17) is:

$$\sigma^2 = \frac{1}{T_0}\int_0^{T_0}\left(R(t) - \bar{R}(t)\right)^2\mathrm{dt} + \frac{1}{T_0}\int_0^{T_0}\left(\bar{R}(t) - \hat{R}(t)\right)^2\mathrm{dt} + \\ + \frac{2}{T_0}\int_0^{T_0}\left(R(t) - \bar{R}(t)\right)\left(\bar{R}(t) - \hat{R}(t)\right)\mathrm{dt} = \sigma_1^2 + \sigma_2^2 + 2\sigma_{12}^2 \tag{22}$$

Each component is calculated separately.

$$\sigma_{12}^2 = \frac{1}{nT}\int_0^{nT}\left(R(t) - \bar{R}(t)\right)\left(\bar{R}(t) - \hat{R}(t)\right)\mathrm{dt} = \\ = \frac{1}{n}\sum_{k=0}^{n-1}\left[\frac{1}{T}\int_{kT}^{(k+1)T}\left(R(t) - \bar{R}(t)\right)\left(\bar{R}(t) - \hat{R}(t)\right)\mathrm{dt}\right] = \\ = \frac{1}{n}\sum_{k=0}^{n-1}\left[\left(\bar{R}_k - \hat{R}_k\right)\frac{1}{T}\int_{kT}^{(k+1)T}\left(R(t) - \bar{R}(t)\right)\mathrm{dt}\right] \tag{23}$$

Equation (23) is the cross-covariance between the forecast error term and the integral difference of the actual and the best scheduled ramping rates. This term should be zero, since presence of any cross-covariance can be used to enhance the forecasting technique. This statement is verified numerically.

Next, σ_2 is calculated as follows:

$$\sigma_2^2 = \frac{1}{nT}\int_0^{nT}\left(\bar{R}(t) - \hat{R}(t)\right)^2\mathrm{dt} = \frac{1}{n}\sum_{k=0}^{n-1}\frac{1}{T}\int_{kT}^{(k+1)T}\left(\bar{R}(t) - \hat{R}(t)\right)^2\mathrm{dt} = \\ = \frac{1}{n}\sum_{k=0}^{n-1}\left(\bar{R}_k - \hat{R}_k\right)^2 = \frac{1}{nT^2}\sum_{k=0}^{n-1}\left[\left(\bar{P}_{k+1} - \bar{P}_k\right) - \left(\hat{P}_{k+1} - \hat{P}_k\right)\right]^2 = \\ = \frac{1}{T^2}\left[\frac{1}{n}\sum_{k=0}^{n-1}\left(\bar{P}_{k+1} - \hat{P}_{k+1}\right)^2 + \frac{1}{n}\sum_{k=0}^{n-1}\left(\bar{P}_k - \hat{P}_k\right)^2 - \right. \\ \left. - \frac{2}{n}\sum_{k=0}^{n-1}\left(\bar{P}_{k+1} - \hat{P}_{k+1}\right)\left(\bar{P}_k - \hat{P}_k\right)\right] \tag{24}$$

Using (18), (24) can be split into load and VER terms:

$$\sigma_2^2 = \frac{1}{T^2}\left[\frac{1}{n}\sum_{k=0}^{n-1}\left(P_{k+1}^L-\hat{P}_{k+1}^L\right)^2+\frac{1}{n}\sum_{k=0}^{n-1}\left(P_k^L-\hat{P}_k^L\right)^2-\right.$$
$$\left.-\frac{2}{n}\sum_{k=0}^{n-1}\left(P_{k+1}^L-\hat{P}_{k+1}^L\right)\left(P_k^L-\hat{P}_k^L\right)\right]+\frac{1}{T^2}\left[\frac{1}{n}\sum_{k=0}^{n-1}\left(P_{k+1}^V-\hat{P}_{k+1}^V\right)^2+\right.$$
$$\left.+\frac{1}{n}\sum_{k=0}^{n-1}\left(P_k^V-\hat{P}_k^V\right)^2-\frac{2}{n}\sum_{k=0}^{n-1}\left(P_{k+1}^V-\hat{P}_{k+1}^V\right)\left(P_k^V-\hat{P}_k^V\right)\right]-$$
$$-\frac{2}{T^2}\left[\frac{1}{n}\sum_{k=0}^{n-1}\left(P_{k+1}^L-\hat{P}_{k+1}^L\right)\left(P_{k+1}^V-\hat{P}_{k+1}^V\right)+\right.$$
$$+\frac{1}{n}\sum_{k=0}^{n-1}\left(P_k^L-\hat{P}_k^L\right)\left(P_k^V-\hat{P}_k^V\right)-\frac{1}{n}\sum_{k=0}^{n-1}\left(P_{k+1}^L-\hat{P}_{k+1}^L\right)\left(P_k^V-\hat{P}_k^V\right)-$$
$$\left.-\frac{1}{n}\sum_{k=0}^{n-1}\left(P_{k+1}^V-\hat{P}_{k+1}^V\right)\left(P_k^L-\hat{P}_k^L\right)\right]=\sigma_{2L}^2+\sigma_{2V}^2-2\sigma_{2LV}^2 \quad (25)$$

where σ_{2LV} is zero according to (16). The first two terms of σ_{2L} are the standard deviation and the third term is the single lag auto-covariance of the load forecast error. Using the forecast error definitions (9) and (10), σ_{2L} and σ_{2V} can be written as:

$$\sigma_{2L} = \frac{1}{T}\varepsilon_L\cdot\sqrt{2\left(1-\rho_L^2\right)}\cdot P_L^{peak} \quad (26)$$

$$\sigma_{2V} = \frac{1}{T}\varepsilon_V\cdot\sqrt{2\left(1-\rho_V^2\right)}\cdot\pi\cdot P_L^{peak} \quad (27)$$

where ρ_L and ρ_V are auto-correlations of load and VER forecast errors respectively.

Finally, the calculation of σ_1 uses normalized profiles of the load and VER output:

$$R^L(t) = \frac{\mathrm{d}P^L(t)}{\mathrm{d}t} = \frac{\mathrm{d}\left(P_0^L(\alpha_L t)P_L^{peak}\right)}{\mathrm{d}t} = R_0^L(\alpha_L t)\cdot\alpha_L\cdot P_L^{peak} \quad (28)$$

$$R^V(t) = \frac{\mathrm{d}P^V(t)}{\mathrm{d}t} = \frac{\mathrm{d}\left(P_0^V(\alpha_V t)\cdot\gamma\cdot\pi\cdot P_L^{peak}\right)}{\mathrm{d}t} =$$
$$= R_0^V(\alpha_V t)\cdot\alpha_V\cdot\gamma\cdot\pi\cdot P_L^{peak} \quad (29)$$

The best schedule profiles are expressed as follows:

$$\bar{R}_T^L(t) = \frac{1}{T^2}\left[\int_{kT}^{(k+1)T}P(\alpha_L t)\mathrm{d}t-\int_{(k-1)T}^{kT}P(\alpha_L t)\mathrm{d}t\right]=$$
$$=\frac{1}{\alpha_L T^2}\left[\int_{k\alpha_L T}^{(k+1)\alpha_L T}P(t)\mathrm{d}t-\int_{(k-1)\alpha_L T}^{k\alpha_L T}P(t)\mathrm{d}t\right]=$$
$$=\frac{1}{(\alpha_L T)^2}\left[\int_{k\alpha_L T}^{(k+1)\alpha_L T}P_0(t)\mathrm{d}t-\int_{(k-1)\alpha_L T}^{k\alpha_L T}P_0(t)\mathrm{d}t\right]\alpha_L\cdot P_L^{peak}=$$
$$=\bar{R}_{T_L}^L(\alpha_L t)\cdot\alpha_L\cdot P_L^{peak} \quad (30)$$

where $T_L\equiv\alpha_L\cdot T$ is the scheduling timestep normalized by the load variability. Similarly derivation for the VER gives:

$$\bar{R}_T^V(t) = \bar{R}_{T_V}^V(\alpha_V t)\cdot\alpha_V\cdot\gamma\cdot\pi\cdot P_L^{peak} \quad (31)$$

Drawing upon (22), the expression for σ_1 with normalized profiles is represented as:

$$\sigma_1^2 = \frac{1}{T_0}\int_0^{T_0}\left(R^L(t)-\bar{R}_T^L(t)\right)^2\mathrm{d}t+\frac{1}{T_0}\int_0^{T_0}\left(R^V(t)-\bar{R}_T^V(t)\right)^2\mathrm{d}t-$$
$$-\frac{2}{T_0}\int_0^{T_0}\left[\left(R^L(t)-\bar{R}_T^L(t)\right)\left(R^V(t)-\bar{R}_T^V(t)\right)\right]\mathrm{d}t=$$
$$=\left(\alpha_L P_L^{peak}\right)^2\frac{1}{T_0}\int_0^{T_0}\left(R^L(\alpha_L t)-\bar{R}_{T_L}^L(\alpha_L t)\right)^2\mathrm{d}t+$$
$$+\left(\alpha_V\gamma\pi\cdot P_L^{peak}\right)^2\frac{1}{T_0}\int_0^{T_0}\left(R^V(\alpha_V t)-\bar{R}_{T_V}^V(\alpha_V t)\right)^2\mathrm{d}t-$$
$$-2\left(\sqrt{\alpha_L\cdot\alpha_V\cdot\gamma\cdot\pi}P_L^{peak}\right)^2\times$$
$$\times\frac{1}{T_0}\int_0^{T_0}\left(R^L(\alpha_L t)-\bar{R}_{T_L}^L(\alpha_L t)\right)\left(R^V(\alpha_V t)-\bar{R}_{T_V}^V(\alpha_V t)\right)\mathrm{d}t=$$
$$=\left(\alpha_L^2\cdot\sigma_{1L}^2+\alpha_V^2\gamma^2\pi^2\cdot\sigma_{1V}^2-2\alpha_L\alpha_V\gamma\pi\cdot\sigma_{1LV}^2\right)\left(P_L^{peak}\right)^2 \quad (32)$$

As mentioned in Section III-A, the calculations of σ_{1L}, σ_{1V} and σ_{1LV} are performed in the spectral domain. Using Parseval's theorem:

$$\sigma_{1L}^2 = \int_{-\infty}^{+\infty}E\left[\left|R^L(\omega)-\bar{R}_{T_L}^L(\omega)\right|^2\right]\mathrm{d}\omega \quad (33)$$

$$\sigma_{1V}^2 = \int_{-\infty}^{+\infty}E\left[\left|R^V(\omega)-\bar{R}_{T_V}^V(\omega)\right|^2\right]\mathrm{d}\omega \quad (34)$$

$$\sigma_{1LV}^2 = \frac{1}{\sqrt{\alpha_V/\alpha_L}}\int_{-\infty}^{+\infty}E\left[\left(R^L(\omega)-\bar{R}_{T_L}^L(\omega)\right)^*\times\right.$$
$$\left.\times\left(R^V\left(\frac{\omega}{\alpha_V/\alpha_L}\right)-\bar{R}_{T_V}^V\left(\frac{\omega}{\alpha_V/\alpha_L}\right)\right)\right]\mathrm{d}\omega \quad (35)$$

where $R(\omega)$ is the truncated Fourier transform of $R(t)$:

$$R(\omega) = \frac{1}{\sqrt{T_0}}\int_0^{T_0}R(t)e^{-j\omega t}\mathrm{d}t \quad (36)$$

The σ_{1LV} term depends on both α_L and α_V. This dependence exists to emphasize the disproportional scaling of the load and VER power spectra. If these variabilities are changed disproportionately, the total variability change depends on the proportion of variabilities α_V/α_L. However, if the goal is to study the impact of the total variability change on the ramping reserve requirement, load and VER variability would change proportionally. In this case, σ_1 only depends on $\alpha\cdot T$ which means that the increase in the variability can be compensated by the decrease of the scheduling timestep. However, in that case the total ramping reserve requirement increases α times. Thus, the ramping reserve requirement is reasonably proportional to the total variability of the system.

The goal now is to express $R^L(\omega)$, $R^V(\omega)$, $\bar{R}_{T_L}^L(\omega)$ and $\bar{R}_{T_V}^V(\omega)$ in terms of $P^L(\omega)$ and $P^V(\omega)$. Since the cases for load and VER are calculated similarly, only one profile is considered and the superscripts L, V are omitted. For the data with resolution T_s, the Fourier transform of the derivative is as

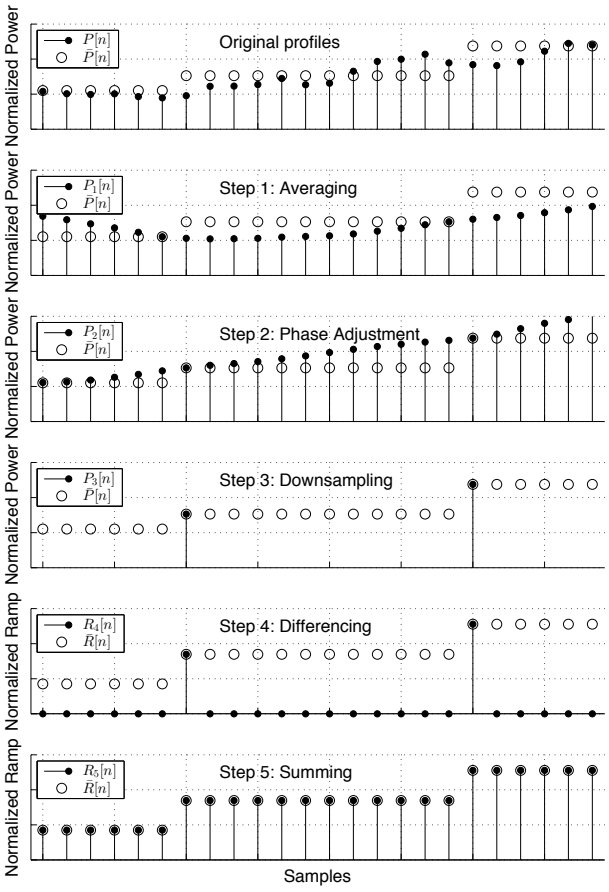

Figure 3: Five steps of time domain processing

follows:

$$R(\omega) = \mathscr{F}\left(\frac{P_k - P_{k-1}}{T_s}\right) = \frac{1}{T_s}P(\omega)\left(1 - e^{-j\omega T_s}\right) \tag{37}$$

The following section is devoted to the time-domain demonstration of the processing steps, which clarifies the logic of the spectral domain manipulations later.

3) Time Domain Demonstration: The transformation from $p[n]$ into $\bar{p}[n]$ has five steps as demonstrated in Fig. 3:

Step 1: Averaging. Averaging calculates the average of the input for one scheduling time step T:

$$P_1[n] = \frac{1}{N}\sum_{k=0}^{N-1} P[n-k] \tag{38}$$

where $N = T_x/T_s$ is the number of samples in T_x. The last samples of each T_x interval match the profile average value for that interval and should be extracted by downsampling the profile with T_x time step. Since the downsampling process starts from the first sample, a phase adjustment of the profile is implemented.

Step 2: Phase Adjustment. Phase adjustment shifts the profile by $N-1$ samples:

$$P_2[n] = P_1[n-(N-1)] \tag{39}$$

Step 3: Downsampling. The profile is downsampled with a time step T_x:

$$P_3[n] = \begin{cases} P_2[n], & n = k\cdot N; \\ 0, & \text{otherwise.} \end{cases} \tag{40}$$

Step 4: Differencing. Differentiation with a step N generates the sampled data for $\bar{R}_{T_x}$:

$$R_4[n] = \begin{cases} \frac{P_3[n]-P_3[n-N]}{T_x}, & n = k\cdot N; \\ 0, & \text{otherwise.} \end{cases} \tag{41}$$

Step 5: Summing. The last step is to turn single samples into rectangles for each interval. Since each interval contains only one non-zero sample, summing the recent N samples for each point in the interval yields the value of the same sample:

$$R_5[n] = \sum_{k=0}^{N-1} R_4[n-k] \tag{42}$$

Fig. 3 shows, that consecutive implementation of these four processing steps convert $p[n]$ into $\bar{p}[n]$. The next paragraph implements these four steps in the spectral domain.

4) Frequency Domain Calculations: The same processing steps described in the previous section are implemented in the spectral domain.

Step 1: Averaging. Using the linearity and translation properties of the Fourier transform, (38) takes the following form in the spectral domain:

$$P_1(\omega) = \frac{1}{N}\sum_{n=0}^{N-1} P(\omega)e^{-j\omega nT_s} \tag{43}$$

Using the formula for the sum of geometric progression:

$$P_1(\omega) = \frac{1}{N}P(\omega)\frac{1-e^{-jN\omega T_s}}{1-e^{-j\omega T_s}} = \frac{1}{N}P(\omega)\frac{1-e^{-j\omega T_x}}{1-e^{-j\omega T_s}} \tag{44}$$

Step 2: Phase Adjustment. Using the translation property of the Fourier transform, (39) takes the following form in the spectral domain:

$$P_2(\omega) = P_1(\omega)\cdot e^{j\omega(N-1)T_s} = \frac{1}{N}P(\omega)\frac{1-e^{-j\omega T_x}}{1-e^{-j\omega T_s}}\cdot e^{j\omega(T_x-T_s)} \tag{45}$$

Step 3: Downsampling. The spectrum of the downsampled profile has the following form:

$$\begin{aligned} P_3(\omega) &= \frac{1}{N}\sum_{n=0}^{N-1} P_2\left(\omega - \frac{2\pi n}{T_x}\right) = \\ &= \frac{1}{N^2}\sum_{n=0}^{N-1}\left[P\left(\omega - \frac{2\pi n}{T_x}\right)\frac{1-e^{-j\left(\omega-\frac{2\pi n}{T_x}\right)T_x}}{1-e^{-j\left(\omega-\frac{2\pi n}{T_x}\right)T_s}}e^{j\left(\omega-\frac{2\pi n}{T_x}\right)(T_x-T_s)}\right] = \\ &= \frac{1}{N^2}\sum_{n=0}^{N-1}\left[P\left(\omega - \frac{2\pi n}{T_x}\right)\frac{1-e^{-j(\omega T_x-2\pi n)}}{1-e^{-j\left(\omega-\frac{2\pi n}{T_x}\right)T_s}}\times\right. \\ &\left.\times\, e^{j(\omega T_x-2\pi n)}e^{j\left(\omega-\frac{2\pi n}{T_x}\right)T_s}\right] = \\ &= \frac{1}{N^2}\sum_{n=0}^{N-1}\left[P\left(\omega - \frac{2\pi n}{T_x}\right)\frac{e^{-j\left(\omega-\frac{2\pi n}{T_x}\right)T_s}}{1-e^{-j\left(\omega-\frac{2\pi n}{T_x}\right)T_s}}\right]\left(1-e^{-j\omega T_x}\right)e^{j\omega T_x} \end{aligned} \tag{46}$$

where $\exp(j2\pi n) = 1$ is taken into account.

Step 4: Differencing. The differenced profile takes the following form in the spectral domain:

$$R_4(\omega) = \frac{1}{T_x} P_3(\omega)\left(1 - e^{-j\omega T_x}\right) = \\ = \frac{1}{T_x N^2} \sum_{n=0}^{N-1} \left[P\left(\omega - \frac{2\pi n}{T_x}\right) \frac{e^{-j\left(\omega - \frac{2\pi n}{T_x}\right)T_s}}{1 - e^{-j\left(\omega - \frac{2\pi n}{T_x}\right)T_s}} \right] \times \\ \times \left(1 - e^{-j\omega T_x}\right)^2 e^{j\omega T_x} \tag{47}$$

Step 5: Summing. Similar to the first step, in the spectral domain (42) takes the following form:

$$R_5(\omega) = R_4(\omega) \cdot \frac{1 - e^{-j\omega T_x}}{1 - e^{-j\omega T_s}} = \\ = \frac{1}{T_x N^2} \sum_{n=0}^{N-1} \left[P\left(\omega - \frac{2\pi n}{T_x}\right) \frac{e^{-j\left(\omega - \frac{2\pi n}{T_x}\right)T_s}}{1 - e^{-j\left(\omega - \frac{2\pi n}{T_x}\right)T_s}} \right] \times \\ \times \frac{\left(1 - e^{-j\omega T_x}\right)^3}{1 - e^{-j\omega T_s}} \cdot e^{j\omega T_x} \tag{48}$$

Thus:

$$\bar{R}_{T_x}(\omega) = \frac{T_s^2}{T_x^3} \cdot \sum_{n=0}^{\frac{T_x}{T_s}-1} \left[P\left(\omega - \frac{2\pi n}{T_x}\right) \times \right. \\ \left. \times \frac{e^{-j\left(\omega - \frac{2\pi n}{T_x}\right)T_s}}{1 - e^{-j\left(\omega - \frac{2\pi n}{T_x}\right)T_s}} \right] \frac{\left(1 - e^{-j\omega T_x}\right)^3}{1 - e^{-j\omega T_s}} \cdot e^{j\omega T_x} \tag{49}$$

5) Simplifications: The final expressions should not depend on the sampling period T_s and the length of the available data N. Equation (49) can be simplified by making reasonable assumptions. First, it is assumed that the data sampling rate is much higher than its variability. Accurate calculations require high resolution data that captures the variability. Since the variability corresponds to the data spectral width, this assumption implies that the data spectral width is much smaller than the sampling rate. As a result, the spectrum has negligible values at $\omega \gtrsim 1/T_s$. Thus, the following simplifications can be made by taking the first order approximation of the Taylor series:

$$1 - e^{-j\omega T_s} \approx j\omega T_s \tag{50}$$

$$e^{-j\omega T_s} \approx 1 \tag{51}$$

The same applies to all shifted spectral copies. Using these simplifications, (37) and (49) can be rewritten as:

$$R(\omega) = j\omega P(\omega) \tag{52}$$

$$\bar{R}_{T_x}(\omega) = \frac{T_s}{T_x^3} \cdot \sum_{n=0}^{\frac{T_x}{T_s}-1} \left[\frac{P\left(\omega - \frac{2\pi n}{T_x}\right)}{j\left(\omega - \frac{2\pi n}{T_x}\right)} \right] \frac{\left(1 - e^{-j\omega T_x}\right)^3}{1 - e^{-j\omega T_s}} \cdot e^{j\omega T_x} \tag{53}$$

The multiplier $1/\left(1 - e^{-j\omega T_s}\right)$ in (53) is a periodic function that matches $1/\omega$ well at low frequencies. Its multiplication by the sum of the shifted spectral copies makes the copies far from the center appear very small. Thus, it can be replaced by $1/\omega$. Also, since $1/\omega$ decays monotonically, it mitigates all the copies outside the range, thus the summation can be done over infinity. This also makes the final expression independent

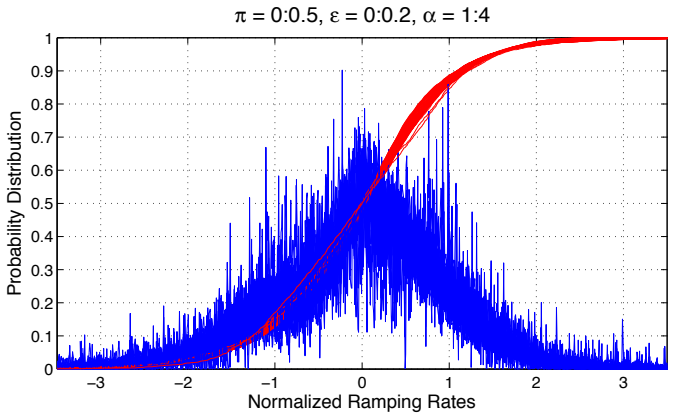

Figure 4: Probability density and cumulative probability functions for different values of π, ε and α

of the sampling frequency:

$$\bar{R}_{T_x}(\omega) = -\frac{1}{T_x^3} \cdot \sum_{n=-\infty}^{+\infty} \left[\frac{P\left(\omega - \frac{2\pi n}{T_x}\right)}{\left(\omega - \frac{2\pi n}{T_x}\right)} \right] \frac{\left(1 - e^{-j\omega T_x}\right)^3}{\omega} e^{j\omega T_x} \tag{54}$$

Equation (54) shows, that the variability and the scheduling time step appear everywhere as multipliers. This means, that the impact of increased variability on the system can be effectively mitigated by reduced scheduling time step. Substituting (54) into (33), (34) and (35), the resulting expression depends on the following components:

$$\rho\left(\omega - \frac{2\pi n}{T_x}, \omega - \frac{2\pi m}{T_x}\right) = E\left[P^*\left(\omega - \frac{2\pi n}{T_x}\right) P\left(\omega - \frac{2\pi m}{T_x}\right)\right] \tag{55}$$

for all values of m and n, which are the samples of the spectrum correlation function. The correlation happens between mixed copies of VER and load spectrum.

C. The Probability Distribution Shape Consideration

Once the standard deviation has been calculated according to Equation (19), the paper returns to the determination of β found in (20). To that end, the probability distribution of (17) is studied, which also allows revising the Assumption 1. This is achieved by varying the probability density of (17) with different values of penetration level, forecast error and variability. Changes in capacity factor and scheduling time step would have similar impact as penetration level and variability respectively [18]. Fig. 4 shows the associated probability density function normalized to unit standard deviation. Here, the family of probability density profiles largely differ from each other and do not have normal shape in contradiction to Assumption 1. However, confidence intervals for the given probabilities are more important in the reserve requirement calculation. Therefore, the associated family of cumulative distribution function (CDF) is represented in Fig. 4. Although there is still a significant difference amongst them, in the scope of this work only the 90% and 95% confidence intervals are of the most interest. As Table I shows, the 90% and 95% confidence intervals generally agree for the wide ranges of penetration level, forecast error and variability. The inaccuracy,

defined here as the ratio of the standard deviation and average value, is comparably very small. Thus, it can be concluded that the reserve requirements for these two confidence intervals are:

$$R_{90\%}^{RAMP} \approx 1.8\sigma \tag{56}$$

$$R_{95\%}^{RAMP} \approx 2.2\sigma \tag{57}$$

where σ is calculated according to (22).

Table I: 90% and 95% confidence intervals

Percentage	Min	Max	Inaccuracy
5%	-1.8010	-1.5554	0.039
95%	1.4493	1.5646	0.018
2.5%	-2.2288	-1.8195	0.036
97.5%	1.7768	1.9955	0.025

IV. CONCLUSIONS AND FUTURE WORK

The framework established in this work allows an assessment of the power system ramping reserve requirement. It is based on analytical derivations of the standard deviation that shows that the reserve requirements depends on non-dimensional parameters of the power system and the net load. This result is contrary to the assumptions in the existing literature. As future research direction, a set of validating simulations will be performed to study the impact of the calculated reserves on the system performance.

REFERENCES

[1] H. Holttinen, M. Milligan, E. Ela, N. Menemenlis, J. Dobschinski, B. Rawn, R. J. Bessa, D. Flynn, E. Gomez-Lazaro, and N. K. Detlefsen, "Methodologies to Determine Operating Reserves Due to Increased Wind Power," *Sustainable Energy, IEEE Transactions on*, vol. 3, no. 4, pp. 713–723, 2012.

[2] E. Ela, B. Kirby, E. Lannoye, M. Milligan, D. Flynn, B. Zavadil, and M. O'Malley, "Evolution of operating reserve determination in wind power integration studies," in *Power and Energy Society General Meeting, 2010 IEEE*, 2010, pp. 1–8.

[3] H. Holttinen, M. Milligan, B. Kirby, T. Acker, V. Neimane, and T. Molinski, "Using Standard Deviation as a Measure of Increased Operational Reserve Requirement for Wind Power," *Wind Engineering*, vol. 32, no. 4, pp. 355–377, 2008.

[4] North American Electric Reliability Corporation, "Reliability Standards for the Bulk Electric Systems of North America," *NERC Reliability Standards Complete Set*, pp. 1–10, 2012.

[5] A. Robitaille, I. Kamwa, A. Oussedik, M. de Montigny, N. Menemenlis, M. Huneault, A. Forcione, R. Mailhot, J. Bourret, and L. Bernier, "Preliminary Impacts of Wind Power Integration in the Hydro-Quebec System," *Wind Engineering*, vol. 36, no. 1, pp. 35–52, Feb. 2012.

[6] T. Aigner, S. Jaehnert, G. L. Doorman, and T. Gjengedal, "The Effect of Large-Scale Wind Power on System Balancing in Northern Europe," *Sustainable Energy, IEEE Transactions on*, vol. 3, no. 4, pp. 751–759, 2012.

[7] B. C. Ummels, M. Gibescu, E. Pelgrum, W. L. Kling, and A. J. Brand, "Impacts of Wind Power on Thermal Generation Unit Commitment and Dispatch," *Energy Conversion, IEEE Transactions on*, vol. 22, no. 1, pp. 44–51, 2007.

[8] D. A. Halamay, T. K. A. Brekken, A. Simmons, and S. McArthur, "Reserve Requirement Impacts of Large-Scale Integration of Wind, Solar, and Ocean Wave Power Generation," *Sustainable Energy, IEEE Transactions on*, vol. 2, no. 3, pp. 321–328, 2011.

[9] P. J. Luickx, E. D. Delarue, and W. D. D'haeseleer, "Effect of the generation mix on wind power introduction," *Renewable Power Generation, IET*, vol. 3, no. 3, pp. 267–278, 2009.

[10] C. W. Hansen and A. D. Papalexopoulos, "Operational Impact and Cost Analysis of Increasing Wind Generation in the Island of Crete," *Systems Journal, IEEE*, vol. 6, no. 2, pp. 287–295, 2012.

[11] Y. V. Makarov, P. V. Etingov, and J. Ma, "Incorporating Uncertainty of Wind Power Generation Forecast Into Power System Operation , Dispatch , and Unit Commitment Procedures," *Sustainable Energy, IEEE Transactions on*, vol. 2, no. 4, pp. 433–442, 2011.

[12] Y. V. Makarov, S. Lu, N. Samaan, Z. Huang, K. Subbarao, P. V. Etingov, J. Ma, R. P. Hafen, R. Diao, and N. Lu, "Integration of Uncertainty Information into Power System Operations," in *Power and Energy Society General Meeting, 2011 IEEE*, 2011, pp. 1–13.

[13] Y. V. Makarov, C. Loutan, J. Ma, and P. de Mello, "Operational Impacts of Wind Generation on California Power Systems," *Power Systems, IEEE Transactions on*, vol. 24, no. 2, pp. 1039–1050, 2009.

[14] B.-M. Hodge, D. Lew, M. Milligan, H. Holttinen, S. Sillanpää, E. Gómez-Lázaro, R. Scharff, L. Söder, X. G. Larsén, G. Giebel, D. Flynn, and J. Dobschinski, "Wind Power Forecasting Error Distributions: An International Comparison," National Renewable Energy Laboratory, Tech. Rep., 2012.

[15] B. Hodge and M. Milligan, "Wind Power Forecasting Error Distributions over Multiple Timescales," in *Power and Energy Society General Meeting, 2011 IEEE*. National Renewable Energy Laboratory, 2011, pp. 1–8.

[16] G. Giebel, R. Brownsword, G. Kariniotakis, M. Denhard, and C. Draxl, "The State-Of-The-Art in Short-Term Prediction of Wind Power: A Literature Overview," ANEMOS.plus, Tech. Rep., 2011.

[17] A. M. Farid and A. Muzhikyan, "The Need for Holistic Assessment Methods for the Future Electricity Grid," in *GCC Power 2013 Conference & Exhibition*, Abu Dhabi, UAE, 2013, pp. 1–13.

[18] A. Muzhikyan, A. M. Farid, and K. Youcef-Toumi, "An Enhanced Method for the Determination of Load Following Reserves," in *American Control Conference 2014 (ACC2014)*, Portland, OR, 2014, pp. 926–933.

[19] ——, "Variable energy resource induced power system imbalances: A generalized assessment approach," in *Technologies for Sustainability (SusTech), 2013 1st IEEE Conference on*, Portland, OR, 2013, pp. 250–257.

[20] ——, "Variable energy resource induced power system imbalances: Mitigation by increased system flexibility, spinning reserves and regulation," in *Technologies for Sustainability (SusTech), 2013 1st IEEE Conference on*, Portland, OR, 2013, pp. 15–22.

[21] S. Frank and S. Rebennack, "A Primer on Optimal Power Flow: Theory, Formulation, and Practical Examples," Colorado School of Mines, Tech. Rep. October, 2012.

[22] C. Wang, Z. Lu, and Y. Qiao, "A Consideration of the Wind Power Benefits in Day-Ahead Scheduling of Wind-Coal Intensive Power Systems," *Power Systems, IEEE Transactions on*, vol. 28, no. 99, p. 1, 2012.

[23] J. Apt, "The spectrum of power from wind turbines," *Journal of Power Sources*, vol. 169, no. 2, pp. 369–374, Jun. 2007.

[24] A. E. Curtright and J. Apt, "The character of power output from utility-scale photovoltaic systems," *Progress in Photovoltaics: Research and Applications*, vol. 16, no. 3, pp. 241–247, May 2008.

[25] C. Monteiro, R. Bessa, V. Miranda, A. Botterud, J. Wang, and G. Conzelmann, "Wind Power Forecasting: State-of-the-Art 2009," Argonne National Laboratory, Illinois, Tech. Rep., 2009.

[26] E. Hirst, "Integrating Wind Energy With the BPA Power System: Preliminary Study," Tech. Rep., 2002.

[27] E. A. Belati and G. R. M. da Costa, "Transmission loss allocation based on optimal power flow and sensitivity analysis," *International Journal of Electrical Power and Energy Systems*, vol. 30, no. 4, pp. 291–295, May 2008.